ELSEVIER

Journal of Alloys and Compounds 271–273 (1998) 826–830

Journal of ALLOYS AND COMPOUNDS

ARPES in strongly correlated 4f and 5f systems: Comparison to the Periodic Anderson Model (PAM)

A.J. Arko[a,*], J.J. Joyce[a], L.E. Cox[a], L. Morales[a], J. Sarrao[a], J.L. Smith[a], Z. Fisk[b], A. Menovsky[c], A. Tahvildar-Zadeh[d], M. Jarrell[d]

[a]*Los Alamos National Laboratory, MS-K764, Los Alamos, NM 87545, USA*
[b]*National High Magnetic Field Laboratory, Florida State University, Tallahassee, FL 32306, USA*
[c]*Natuurkundig Laboratorium, University of Amsterdam, Valckenierstraat 65, 1018 XE Amsterdam, The Netherlands*
[d]*University of Cincinnati, Cincinnati, OH 45221-0011, USA*

Abstract

The electronic structure of both Ce and U heavy fermions appears to consist of extremely narrow, nearly temperature-independent bands (i.e., no spectral weight loss or transfer with temperature). A small dispersion of the f-bands above the Kondo temperature is easily measurable so that a Kondo resonance, as defined by NCA, is not evident. Preliminary results, however, indicate that the Periodic Anderson Model (PAM) captures some of the essential physics. Angle-integrated resonant photoemission results on δ-Pu indicate a narrow 5f feature at E_F, similar in width to f-states in Ce and U compounds, but differing in that PES cross-section as a function of $h\nu$ suggests substantial 6d admixture. © 1998 Elsevier Science S.A.

Keywords: Heavy fermions; Electronic structure; Periodic Anderson Model (PAM); Narrow f-bands

1. Introduction

While U and Ce heavy fermion compounds display nearly identical bulk properties [1], photoelectron spectroscopy (PES) on polycrystalline specimens indicated possible fundamental differences since the near-E_F 5f feature, as observed [2] in resonant PES, appeared to be much broader than the corresponding 4f feature; indeed, much broader even than the 5f density of states (DOS) predicted by band calculations [3]. Further, while a typical Ce heavy fermion spectrum showed several 4f features, identified within a Kondo picture [4] as (i) the 'main' or f^0 peak at ≈ -2 eV (also called the charge transfer peak), (ii) the Kondo resonance, i.e. the KR or $4f_{5/2}$, at E_F, and (iii) the Kondo sideband, or the $4f_{7/2}$, at ≈ -0.28 eV, a typical U spectrum measured at resonance in polycrystals showed [2] only a broad featureless triangular structure pinned at E_F. This led to the unsatisfactory situation whereby the single impurity model [5] (SIM) is used to explain Ce compounds (but fails even there to explain single-crystal PES data [6–12]), while identical behavior in U compounds requires another, as yet undeveloped model.

Angle-resolved photoemission (ARPES) data on high-quality single crystals, however, now indicate that these differences are perhaps only quantitative rather than qualitative, and that narrow dispersive f-bands are observed in both 4f and 5f materials both above and below the characteristic Kondo temperature, T_K. Moreover, these measurements [6–12] consistently find substantive disagreements with predictions of the Non-Crossing Approximation [13] (NCA) and Gunnarsson-Schonhammer [14] solution of the SIM. Most notably, the temperature dependence is far too small, or non-existent, while the spectral weights and widths of the f-features do not scale with T_K (indeed, they are totally unrelated to T_K) in contradiction to SIM predictions [13,14]. We are aware of differing views, but in every report where experimental agreement with the SIM is claimed, we can point [6–12] to questionable data, questionable analysis, or both. Besides, the juggling of parameters to reproduce an experimental spectrum for a single material is of no consequence if the predicted trends for a wide range of materials are non-existent.

*Corresponding author. Tel.: (1-505) 665-0758; fax: (1-505) 665-7652; e-mail: arko@lanl.gov

PII: S0925-8388(98)00227-8

2. Theoretical considerations

While several theoretical approaches [15–21] hold promise of accounting for dispersive behavior, we focus below on the periodic Anderson Model [15,16], PAM, which in its preliminary stages appears to capture the essential physics. Quite possibly these different approaches, mostly based on the Anderson Hamiltonian, may eventually converge on the same final result, namely some form of renormalized bands [17,18] displaying minimal temperature dependence. A necessary flattening of these bands at E_F with temperature, due to the correlations, yields the heavy electron masses well as a mimicking, in parts of the Brillouin zone, of the feature called the Kondo resonance.

The PAM is believed to most correctly describe the strong correlation of electrons in Kondo lattice systems; i.e., stoichiometric compounds with 4f or 5f electrons in the valence shell. While for more than a decade the SIM has been the paradigm for comparison with PES, it cannot account for the coherent nature of electrons (i.e., periodic Bloch states) now observed both above and below T_K. The PAM accounts for these effects. Unfortunately, the difficult nature of PAM calculations necessitates the use of simple generic models rather than real systems. Indeed, the calculation is done in infinite dimensions. Nevertheless the predicted trends hold the promise of much better agreement with PES data.

The PAM Hamiltonian on a D-dimensional hypercubic lattice is,-

$$H = \frac{-t^*}{2\sqrt{D}} \sum_{\langle i,j\rangle\sigma} (d^\dagger_{i\sigma} d_{j\sigma} + h.c.) + \sum_{i\sigma} (\varepsilon_d d^\dagger_{i\sigma} d_{i\sigma} + \varepsilon_f f^\dagger_{i\sigma} f_{i\sigma}) + V \sum_{i\sigma} (d^\dagger_{i\sigma} f_{i\sigma} + h.c.) + \sum_i U(n_{fi\uparrow} - 1/2)(n_{fi\downarrow} - 1/2).$$

In the above equation, $d(f)^{(\dagger)}_{i\sigma}$ destroys (creates) a $d(f)$-electron with spin σ on site i. The hopping is restricted to the nearest neighbors and scaled as $t=t^*2\sqrt{D}$. We choose $t^*=1$, the width of the Gaussian density of states, as the energy scale. The unhybridized d-bandwidth is $2\sqrt{D}$, and this broadens further with hybridization. U is the screened on-site Coulomb repulsion for the localized f-states and V is the hybridization between d- and f-states. This model, then, retains the screening and moment formation of the impurity problem, but is further complicated by the lattice effects and the interaction between the moments.

Metzner and Vollhardt [22] observed that the irreducible self-energy and the vertex functions become purely local as the coordination number of the lattice increases. As a consequence, the solution of this interacting lattice model may be mapped onto the solution of a local correlated impurity coupled to an effective bath which is self-consistently determined [23,24]. The Quantum Monte Carlo (QMC) algorithm of Hirsch and Fye [25] is employed to solve the remaining impurity problem. The basic outputs of this procedure are the f and d Green's functions of the model in Matsubara frequency. The maximum entropy method (MEM) is then employed to analytically continue these functions to real frequency [26].

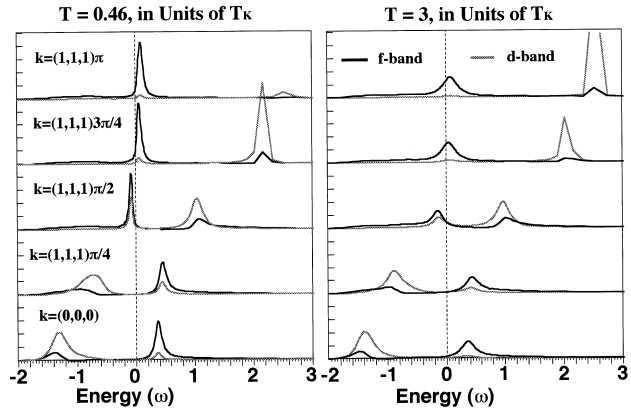

Fig. 1. PAM-derived spectral functions at the indicated points in the simple cubic Brillouin zone, for two temperatures relative to T_K. Dark lines indicate partial f-DOS while gray lines indicate partial d-DOS. Note that the narrowest features, both f and d, are at the Fermi energy.

Initial results indicate a substantial differences between the PAM and the SIM approaches, especially in the much slower temperature dependence of the PAM [15,16]. While both yield a sharp peaking of the DOS at E_F that can be interpreted as a Kondo resonance, the PAM calculations find that these are narrow bands both above and below T_K, as shown in Fig. 1. Here we present the spectral functions for various **k**-vectors in a generic simple cubic zone along the cube diagonal, at two different temperatures ($0.46T_K$ and $3T_K$). A d-band at 0.6 filling is allowed to hybridize with a band of singly occupied f-states, resulting in the two f–d mixed renormalized bands, with a clear hybridization gap. For this system, $U=1.5$, hybridization $V=0.6$, while $T_K=0.02$, in units of t^*. Clearly dispersion is much larger than T_K. There is no f-intensity at E_F for $k=(0,0,0)$, the latter developing only at $k=(1,1,1)\pi/2$. As the temperature increases to $3T_K$ there is only a minimal transfer of spectral weight from the quasiparticle peaks to the 'main' or f^0 peak (still slightly visible at $\omega\approx-1$) in contrast to the SIM. Instead one finds primarily a broadening of the quasiparticle peaks [15,16], very much in accordance with experimental results reported previously [6–12]. Calculations for $T=10T_K$ yield similar results. As in the SIM, the f^0 peak, despite much reduced intensity, is found to increase with decreasing hybridization, and hence T_K.

3. Experimental results and discussion

While the parameters in the above calculations most correctly apply to strongly hybridized ($T_K\approx1200$ K) cubic Ce systems, the predicted trends (i.e., much slower temperature dependence than in the SIM, much more weight at

E_F for a given T_K, much stronger hybridization, dispersion much larger than T_K, etc.) are applicable even to relatively low-T_K materials. Indeed, our first observations [8] of periodic effects above T_K were in cubic $CePt_{2.2}$ ($T_K<20$ K, sample temperature during measurement $T_m\approx120$ K) where the strongest $4f_{5/2}$ signal was obtained for $\mathbf{k}\|(1,1,1)$, and the weakest for $\mathbf{k}\|(1,0,0)$. These results were followed [9] by measurements in the more strongly hybridized $CeBe_{13}$ ($T_K\approx400$ K) where again the weakest signal was for $\mathbf{k}\|(1,0,0)$ and the strongest for $\mathbf{k}\|(1,1,1)$. However, for experimental reasons actual dispersion was not substantiated in those systems. For this reason we show in Fig. 2 ARPES data for tetragonal $CeSb_2$, a ferromagnet below 10 K with an estimated T_K of ≈3 K, where we observed clear evidence of dispersion [11] at $T_m\approx20$ K$\approx10T_K$. The two sets of data in Fig. 2 were taken on different samples at different times. Although LEED was not used for determination of orientation owing to rapid surface deterioration, it is clear that the two data sets represent two different directions in the zone starting from the surface normal, or the Γ-point. In one case (Fig. 2a) the dispersion is toward lower energies, and the rapid decrease of signal strength is now understood as due to a loss of f-admixture in the band below E_F. In the other case (Fig. 2b) the band apparently disperses and flattens out just above E_F, and one can see that the f-intensity remains strong despite a large shift of the $4f_{5/2}$ toward E_F. This data set, then, is understood within the PAM where, unlike in the SIM, a Kondo band of bandwidth $W\gg T_K$ flattens out just above E_F, and exists even at $T>10T_K$.

Similar narrow 5f-bands are also found in uranium systems as seen in the data from a cleaved crystal of antiferromagnetic, tetragonal, USb_2 ($T_N\approx200$ K, $T_m\approx20$ K, $h\nu=35$ eV, $\Delta E=40$ meV). The f-character of bands A and B is deduced from the $h\nu$-dependence [27] of their intensity in the left frame where ARPES data at 13° from the c-axis are shown. Only the f-cross-section increases in this $h\nu$ range [27] while the d-cross-section decreases, so that features A and B are unquestionably f-related. Note the strong dispersion of band B with $h\nu$ in the left frame (≈600 meV across the zone) which is actually quite different from Ce compounds in its strong dispersion. The similarity to Ce occurs in the near-E_F band A whose 20–30 meV of dispersion are more readily seen in the right frame of Fig. 3. Although not evident from Fig. 3, the intensity of the band A quasiparticle peaks drops off dramatically near the c-axis, just as occurs in cubic Ce compounds at the zone center [9], most likely again due to a loss of f-character as it disperses below E_F. The exact strength of the dispersion is masked somewhat by band B which is degenerate with band A near the c-axis, $q=0°$. All this would suggest that the strong correlations are confined to band A and energies very close to E_F.

A most interesting set of ARPES data [11] are shown in Fig. 4, taken in the a–c plane on a cleaved crystal of UPt_3 with a surface normal parallel to the c-axis (here $T_K=10$ K, $T_m\approx20$ K, $h\nu=40$ ev, $\Delta E=40$ meV). Several f-related features are observed, again determined to be so from the cross-section dependence on $h\nu$, as well as from data at the 5d absorption edge (resonance). Any d-derived features at E_F are again of negligible intensity. Features A and B disappear between $\theta=2°$ and $\theta=3.5°$ analyzer angle. This is precisely where band calculations predict [28] that two f-bands cross E_F. Indeed, band calculations predict the existence of features A, B, C and D, although the experimental bands appear to be flatter than the calculated bands (our resolution is insufficient to quantify this). The inset of Fig. 4 compares data at $\theta=1°$ and 25° to emphasize dispersion, though, based on LDA, it is possible that these are actually two different bands. Since $T_m\approx2T_K$ we are again dealing with flat f–d hybridized bands above T_K, just as in Ce compounds.

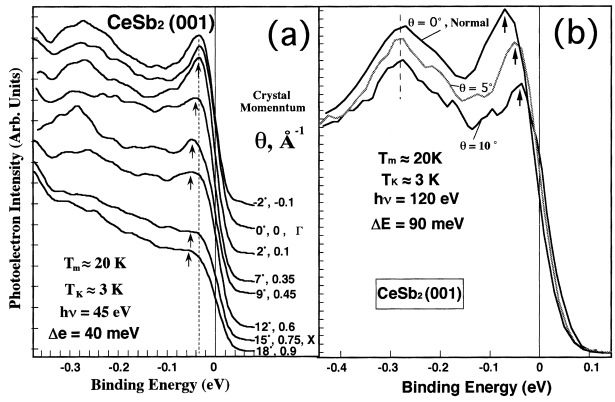

Fig. 2. ARPES spectra for $CeSb_2$, with all analyzer angles measured relative to the surface normal, i.e. (001). (a) Spectra with k_{11} along the (100) direction are shown for $h\nu=40$ eV. Note the dispersion to energies below E_F. (b) Spectra taken along a different direction, possibly along (110), show dispersion toward higher energies. Note that the 4f-spectral weight remains strong as the f-band flattens out just above E_F.

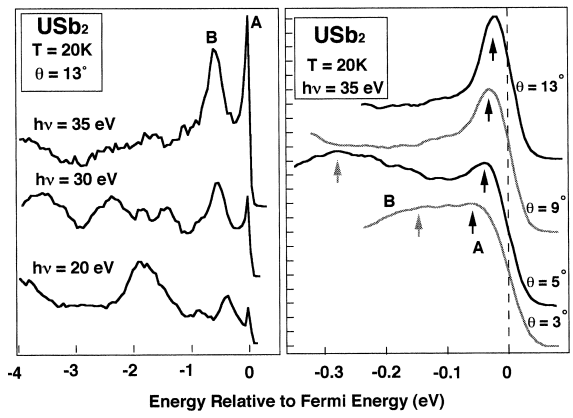

Fig. 3. ARPES spectra for USb_2, with all analyzer angles measured relative to the surface normal, i.e. (001). (a) Spectra at indicated photon energies, but at constant 13° from normal. Note the rapid growth of intensity for features A and B, indicating f-character. (b) Spectra at $h\nu=35$ eV but at varying analyzer angles, to show dispersion of band A.

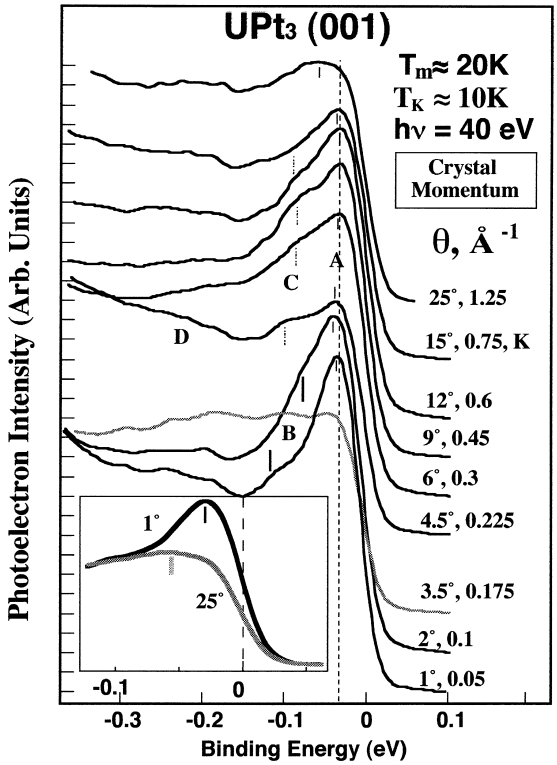

Fig. 4. ARPES spectra at $h\nu$=40 eV and T=20 K for UPt_3 at the indicated points in the Brillouin zone. The data, taken at $2\times T_K$, show huge variation with momentum. Note the sudden disappearance of peak A at 3.5°, precisely where LDA predicts dispersion above E_F. Inset emphasizes the dramatic difference in both peak position and intensity between 1° and 25°.

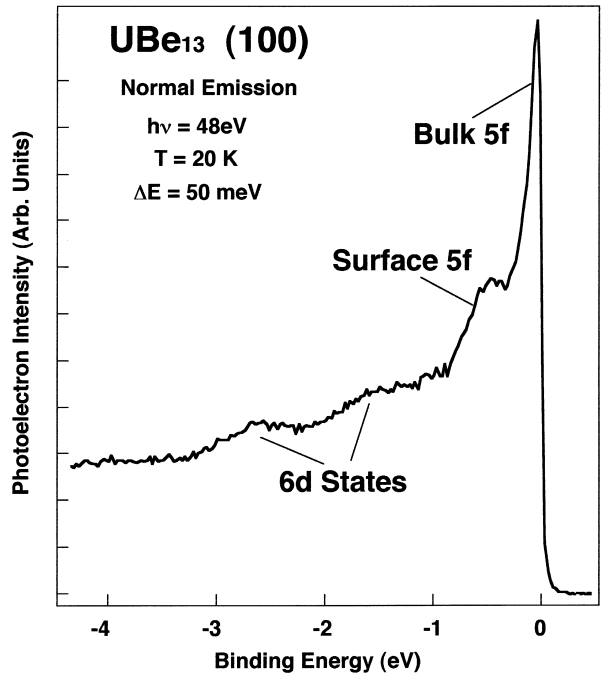

Fig. 5. Normal emission spectrum of UBe_{13} at $h\nu$=48 eV. The feature at −0.5 eV was observed to disappear with 1 Langmuir of oxygen doping [29], and is thus presumed to be due to the surface. Only the 6d states display actual dispersion.

From the above one is led to the conclusion that the electronic structure of both Ce and U compounds is dominated by the existence of extremely narrow f-bands at the Fermi energy, and this already above the characteristic T_K. Temperature dependence studies to 300 K in Ce, Yb, and U compounds [6–12] show that these bands are nearly temperature independent with no spectral weight loss, although there is broadening of the features [10,12] and loss due to truncation by the 300 K Fermi function. While for very low-T_K materials, or, equivalently, for very high temperatures, the PAM and SIM results again converge, in order to understand why the f-bands in $CeSb_2$ and $CePt_{2.2}$ remain strong even above 80 K, one must assume that hybridization parameters, as determined from the SIM, are grossly underestimated.

Very weakly hybridized compounds such as UBe_{13} and UAl_2 remain a puzzle. In both cases most of the f-intensity is concentrated in the moderately narrow intense peak near the Fermi energy (see the normal emission UBe_{13} (100) ARPES spectrum in Fig. 5) with no clear evidence of dispersion, while the temperature dependence (not shown) is nevertheless minimal and no different from high-T_K compounds. The broad feature at −0.5 eV in Fig. 5 is also of f-symmetry, but is clearly surface-related since it rapidly diminishes with surface contamination [29]. While there is much speculation about the possibility of multichannel Kondo phenomena responsible for the non-Fermi-liquid UBe_{13} properties, our data cannot shed much light on this since the relatively broad, dispersionless nature of the 5f peak can also result from disorder.

We have also obtained the first ever spectra at resonance for δ-Pu using our newly-commissioned laser plasma light source, more fully described in [30]. In Fig. 6 (bottom spectrum) we show this data taken at $h\nu$=111 eV and compare it to spectra taken at lower photon energies using a helium resonance lamp. There is recent speculation that δ-Pu is a heavy fermion material [31]. However, while a sharp 5f-related feature is indeed evident at the Fermi energy similar to those in Ce and U heavy fermions, the PES cross-section would indicate a substantial 6d admixture for this feature [27]. This is evidenced by the fact that the broad peak at −1.7 eV grows more rapidly with photon energy relative to the near $-E_F$ feature. This behavior appears consistent with recent band calculations [32] which predict that the broad −1.7 eV peak is derived from nearly localized pure 5f states, while the near-E_F peak is indeed strongly f–d hybridized. In its present form, the PAM is unable to contribute to the understanding of δ-Pu.

Preliminary results from the PAM calculations, then, suggest that the previous discrepancies encountered between experimental ARPES data and the SIM are substantially diminished with the inclusion of the lattice. The weak temperature dependence, as well as dispersion far above T_K is theoretically reproduced, so that PAM is

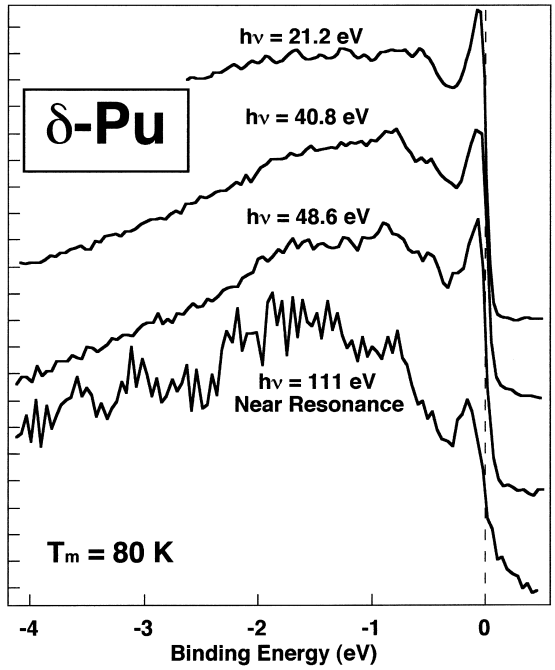

Fig. 6. Angle-integrated spectra of δ-Pu at the indicated photon energies. The near-resonance spectrum at $h\nu$=111 eV was taken with light from a laser plasma light source. The spectral weight of the near-E_F peak increases slower with $h\nu$ than the feature at −1.7 eV and is thus assumed to contain 6d admixture in the DOS. The −1.7 eV feature is believed to be due to nearly localized 5f states.

clearly on the right track. However, we cannot yet, on the basis of the present data, rule out other models which are not yet sufficiently developed to make spectral predictions as detailed as the SIM or the PAM. Both the charge polaron model of Liu [20] and the two-electron band model of Sheng and Cooper [21] can predict many of the bulk properties. In both models the main parameter is the bandwidth of the weakly hybridized f-bands situated near E_F in the ground state. A source of discrimination may be the f^0 peak which is not obtained in [20,21], but may nevertheless occur as a satellite of the photoemission process. The only model that can almost certainly be ruled out is the SIM. Several researchers [33–35] are now starting to use single crystals and finding band behavior at temperatures presumed appropriate for the SIM. The use of scraped polycrystals will most definitely preclude this observation in PES, even at 5 meV resolution [36], especially if the data is further compromised by questionable analysis.

Acknowledgements

Work supported by the US Department of Energy. Part of work done at SRC, which is supported by the NSF under award no. DMR-95-31009.

References

[1] G.R. Stewart, Rev. Mod. Phys. 56 (1984) 755.
[2] J.W. Allen, et al., Phys. Rev. Lett. 54 (1985) 2635.
[3] R.C. Albers, et al., Phys. Rev. B 33 (1986) 8116.
[4] F. Patthey, et al., Phys. Rev. B 35 (1987) 5903.
[5] K.A. Gschneider, Jr., L. Eyring, S. Huffner (Eds.), Handbook on the Physics and Chemistry of Rare Earths, Vol. 10, North Holland, Amsterdam (1987).
[6] J.J. Joyce, et al., Phys. Rev. Lett. 68 (1992) 236.
[7] J.J. Joyce, et al., Phys. Rev. Lett. 72 (1994) 1774.
[8] A.B. Andrews, et al., Phys. Rev. B 51 (1995) 3277.
[9] A.B. Andrews, et al., Phys. Rev. B 53 (1996) 3317.
[10] J.J. Joyce, et al., Phys. Rev. B 54 (1996) 17515.
[11] A.J. Arko et al., Phys. Rev. B 56 (1997) (rapid comm.).
[12] A.J. Arko, et al., Physica B 230–232 (1997) 16.
[13] N.E. Bickers, et al., Phys. Rev. B 36 (1987) 2036.
[14] O. Gunnarson, K. Schonhammer. In: K.A. Gschneider, Jr., L. Eyring, S. Huffner (Eds.), Handbook on the Physics and Chemistry of Rare Earths, Vol. 10, Elsevier Publishers, Amsterdam (1987) pp. 103–163.
[15] A.N. Tahvildar-Zadeh, et al., Phys. Rev. B 55 (1997) R3332.
[16] A.N. Tahvildar-Zadeh et al., Phys. Rev. Lett., in press.
[17] G. Zwicknagl, Advan. Phys. 41 (1992) 203.
[18] M.M. Steiner, et al., Phys. Rev. Lett. 72 (1994) 2923.
[19] S.H. Liu. In: K.A. Gschneider, Jr., L. Eyring, (Eds.), Handbook on the Physics and Chemistry of Rare Earths, Vol. 17, Ch. 111, North Holland, Amsterdam (1993) pp. 87–148.
[20] S.H. Liu, Physica B 240 (1997) 49.
[21] Q.G. Sheng, B.R. Cooper, Phil. Mag. Lett. 72 (1995) 123.
[22] W. Metzner, D. Vollhard, Phys. Rev. Lett. 62 (1989) 324.
[23] T. Pruschke, et al., Adv. in Phys. 42 (1995) 187.
[24] A. Georges, et al., Rev. Mod. Phys. 68 (1996) 13.
[25] J.E. Hirsch, R.M. Fye, Phys. Rev. Lett. 56 (1989) 2521.
[26] M. Jarrell, J. Gubernaitis, Phys. Reports 269(3) (1966) 133.
[27] J.J. Yeh, I. Lindau, Atom. Dat. and Nuc. Tabl. 32 (1985) 1.
[28] R.C. Albers, et al., Phys. Rev. B 33 (1986) 8116.
[29] R.I.R. Blyth, A.B. Andrews, A.J. Arko, J.J. Joyce, P.C. Canfield, Z. Fisk, U.G.L. Lahiase, L. Delong, Surface Review and Letters 1 (1994) 3.
[30] J.J. Joyce, et al., Surface and Interface Analysis 26 (1998) 121.
[31] S. Meot-Reymond, J.-M. Fournier, J. Alloys and Compounds 232 (1996) 119.
[32] J. Wills, O. Eriksson, pers. comm.
[33] D. Vasumathi, et al., Phys. Rev. B 55 (1997) 11714.
[34] C.G. Olson, pers. comm.
[35] H. Kumigashira, et al., Phys. Rev. B 55 (1997) R3355.
[36] M. Garnier, Phys. Rev. Lett. 78 (1997) 4127.